

MULTI-WAVELENGTH OBSERVATIONS OF STELLAR FLARES

P. B. BYRNE

Armagh Observatory, Armagh BT61 9DG, N. Ireland

Abstract. We present observational data on stellar flares from a range of wavelength regimes, many of which were obtained simultaneously. Physical parameters of these flares are derived and discussed in the framework of the general solar flare model. It is found that flares on dMe stars are solar-like, except in mean energy. The parameters of flares on RS CVn stars are more extreme, however, and may require new models for their interpretation.

1. Introduction

Since, in the study of stellar flares, we cannot resolve the phenomenon spatially, simultaneous observations over as many wavelength regions as possible make a vital contribution to our understanding of the event. As a result of improvements in instrumental design these observations can now cover the electromagnetic spectrum from microwaves to X-rays.

I would like to stress at the outset the amount of effort required in acquiring simultaneous data with these instruments. Obtaining good coverage of a star over the entire range of accessible wavelengths requires worldwide collaborations, especially in respect of ground-based data. Extensive collaborations have been built up over the last decade and I would like to take this opportunity to pay tribute to many observers who have taken time out from other work to assist in obtaining the best possible coverage. In spite of these efforts many of the datasets I shall describe are incomplete in their wavelength coverage.

By its very nature it is difficult to organise a review of this type in a way which will be acceptable to all. So the following scheme is a personal one. I have chosen to highlight one or other of the wavelength regions covered in each set of observations, in order of increasing wavelength, so that I can summarize the main conclusions to be derived from that particular energy domain. As a result, the same dataset will sometimes be discussed from different points of view and in different places in the review.

2. X-Ray Flares

One of the primary characteristics of a solar flare is its X-ray signature, while that of the stellar flare has been its broadband optical continuum emission. For this reason a great deal of effort has been expended to establish the relationship between the optical and X-ray emission in stellar flares. A recent, excellent example of this type of observation has been the joint observation of a soft X-ray flare on the star BY Dra by the EXOSAT LE detector and simultaneous *UBVRI* photometry (de Jager *et al.*, 1988). Figure 1 is taken from this work. The following points should be noted. First, the peak of the broadband optical emission precedes that of the soft X-rays by between 4 and

Solar Physics **121**: 61–74, 1989.

© 1989 Kluwer Academic Publishers. Printed in Belgium.

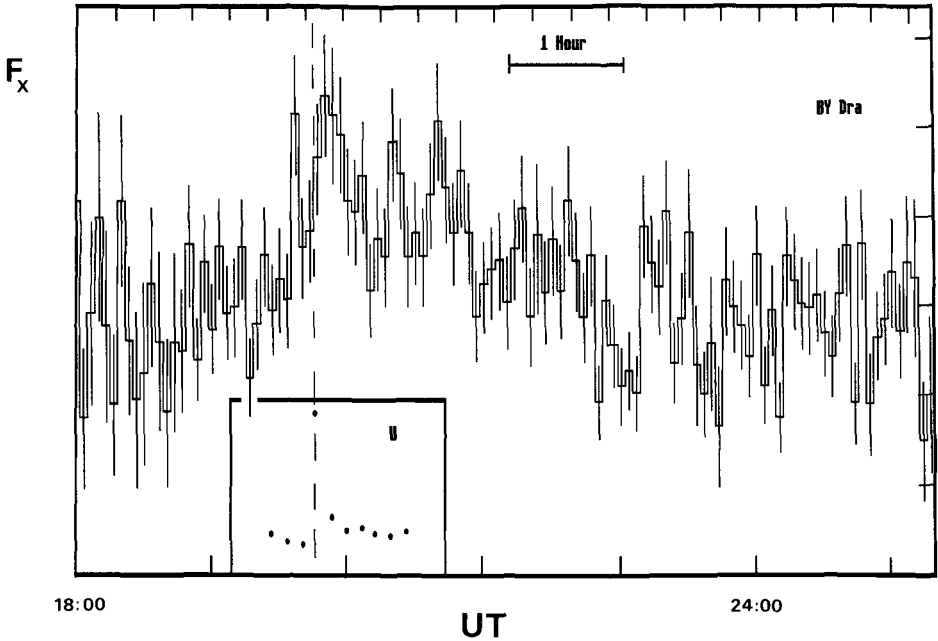


Fig. 1. A simultaneous optical and soft X-ray observation of a flare on the dMe star, BY Dra (de Jager *et al.*, 1988). The histogram shows the EXOSAT soft X-ray data, while the dots indicate the optical U -band light curve. The vertical dashed line is at the time of U -band maximum.

8 min (the resolution of the X-ray data is ≈ 4 min). Second, the time-scale of the optical flare ($\tau_{\text{rise}} \approx 1$ min, $\tau_{\text{fall}} \approx 5$ min) is very much shorter than that of the soft X-rays ($\tau_{\text{rise}} \approx 10$ min, $\tau_{\text{fall}} \approx 1$ hour). Some of the characteristics of this flare are given in Table I. Note that $E_{\text{opt}} \approx E_X$.

Doyle *et al.* (1988a) observed another X-ray flare with the EXOSAT satellite on the star Gliese 644 (Wolf 630) which was recorded in both the soft (LE) and medium (ME) energy detectors (Figure 2). Here we see that the soft X-rays (LE) lag those of medium energy (ME) by ≈ 80 s. A thermal brehmsstrahlung fit to the ME data indicates that this reflects a cooling of the flare from $\approx 5 \times 10^7$ K to $\approx 2.5 \times 10^7$ K during the decay. This event was also observed in $H\alpha$, which exhibited broadening (see below). The ratio of the total energy radiated in soft X-rays to that in $H\alpha$ is ≈ 25 , not very different from that observed in solar flares (Neidig, 1989). Using the approximate relationships for stellar flares that $E_{\text{Balmer}} \approx 3E_{H\alpha}$ and $E_{\text{opt}} \approx 10E_{\text{Balmer}}$ yields $E_{\text{opt}} \approx 1.2E_X$.

In contrast to these results on the ratio of E_{opt}/E_X , EINSTEIN X-ray and simultaneous optical observations of a flare on YZ CMi by Kahler *et al.* (1982) indicate $E_{\text{opt}} \approx 0.7E_X$. An optical flare on YZ CMi observed by Doyle *et al.* (1988b) was initially reported to have no accompanying soft X-ray flare. A re-analysis of this data (Butler, Rodono, and Foing, 1989) has detected the X-ray event and indicates $E_{\text{opt}}/E_X \approx 0.1$.

It would appear, therefore, that there is no unique value for E_{opt}/E_X but that it varies from flare to flare. Nevertheless, values of between ≈ 0.1 and ≈ 1 are representative.

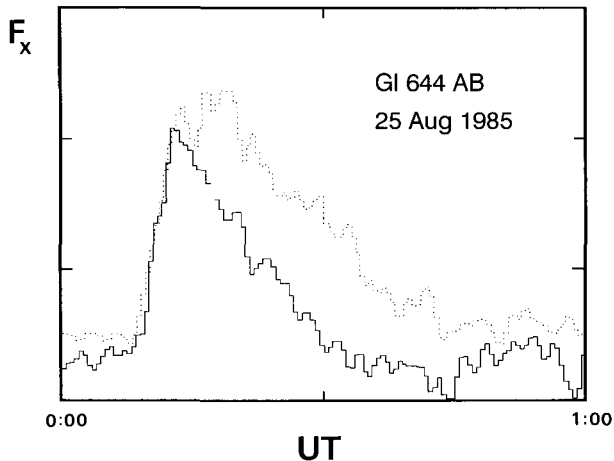


Fig. 2. EXOSAT light curves of a flare on Gliese 644 (Wolf 630) adapted from Doyle *et al.* (1988a). The dotted curve is the soft X-ray ($\approx 0.02\text{--}4$ keV) light curve, while the solid curve is that for the medium energy X-rays ($\approx 2\text{--}8$ keV).

Thus optical continuum emission is a very important part of the energy balance in stellar flares, being of the same order of importance as the soft X-ray emission.

Table I summarizes some of the main X-ray characteristics of representative stellar flares. Plasma temperatures of between 1×10^7 and 5×10^7 K are typical, not very different from large solar flares (Tanaka *et al.*, 1983). In general, temperatures are higher during the rise phase or at peak than later during the decay. Soft X-ray emission measures range from $10^{51}\text{--}10^{53}$ cm $^{-3}$, the lower end of which is comparable to those found in the largest solar two-ribbon flares but extending to larger values.

Electron densities, N_e , can be derived from the X-ray light curve decay times, τ_{decay} , if a simple form of cooling the flare plasma is assumed. Most authors assume either pure radiative cooling or equal contributions from cooling and conduction. Simultaneous observations of a solar flare by EINSTEIN and SMM (Schmitt, Lemen, and Zarro, 1989) indicate that the latter was a good approximation in that instance. In Table I we give electron densities based on the assumption of radiative cooling using the expression (Doyle *et al.*, 1988a)

$$N_e = \frac{3kT}{\Lambda(T)\tau_r},$$

where $\Lambda(T)$ is the plasma emissivity and τ_r is the e^{-1} decay time. Using the values in Doyle *et al.* this expression reduces to

$$N_e = \frac{7.5 \times 10^{14}}{\tau_r}.$$

Values derived in this way are typically $10^{11}\text{--}10^{12}$ cm $^{-3}$, similar to those obtained for the Sun.

Table I also contains entries for two flares observed on RS CVn stars. All of the characteristics of these flares, with the exception of the electron densities, are larger than

TABLE I

Summary of X-ray flares on dMe and RS CVn stars. E_X and E_{opt} are integrated flare energies in the soft X-ray (≈ 0.1 –2 keV) and broad-band optical (Johnson *UBV*), respectively

Star	Source	Temperature (10^7 K)	E_X (10^{32} erg)	E_{opt} (10^{32} erg)	EM (10^{52} erg)	N_e (10^{11} cm $^{-3}$)
dMe flares observed with EXOSAT						
BY Dra	de Jager <i>et al.</i> , 1988	1	20	40	1.2	
EQ Peg	Haisch <i>et al.</i> , 1987	2.6 (rise)	5	(0.16) (Mg II)	1.5	2
		1.4 (decay)				
	Kundu <i>et al.</i>	4.4 (peak)	100	–	20	4
		2.7 (decay)				
Wolf 630	Doyle <i>et al.</i> 1988a	5 (rise)	12	(0.6) (H α)	3	8
		2.5 (decay)		[20]		
dMe flares observed with EINSTEIN						
YZ CMi	Kahler <i>et al.</i> , 1982	2 (peak)	0.36	0.12 (<i>U</i>) [≈ 0.3 (<i>UBV</i>)]	0.5	1
Prox Cen	Haisch <i>et al.</i> , 1981	1.7 (rise)	0.1	–	0.1	1.4
		1.2 (decay)				
	Haisch <i>et al.</i> , 1983	2.7 (peak)	0.35	–	0.1	5
RS CVn flares observed with EXOSAT						
Algol	van den Oord <i>et al.</i> , 1986	5.8 (peak)	250	–	94	2.6
σ Cor Bor	van den Oord <i>et al.</i> , 1988	9.5 (rise)	10^4	–	57 (peak)	9
		6.4 (peak)			23 (rise)	

in the dMes discussed so far. It is clear that flares on these binary subgiant stars are about two orders of magnitude larger than in the dwarf M stars. Clearly, while it may be possible to apply the solar model to the dMe X-ray flares in a relatively straightforward way, more caution must be exercised when dealing with the RS CVns.

3. UV Line Emission

Early attempts to record the ultraviolet spectra of stellar flares were frustrated by a lack of sensitivity. With the advent of the International Ultraviolet Explorer (IUE) it became possible to record dMe and RS CVn ultraviolet spectra with sufficiently high sensitivity and spectral resolution to begin studying stellar flares in a systematic way.

The mid-UV signature of a stellar flare is well illustrated by a flare recorded by IUE on FK Aqr (Gliese 867A) by Butler *et al.* (1981) and shown in Figure 3. The figure shows the spectrum of the star in quiescence and during a 1 hour exposure during which the flare occurred. The dramatic enhancement of all of the chromospheric and transition region lines is apparent. This spectrum also illustrates the limitations of IUE for the study of stellar flares. In order to get an adequately exposed spectrum of the non-flaring star, exposures of the order 20–60 min are necessary. Furthermore, the dead-time to the

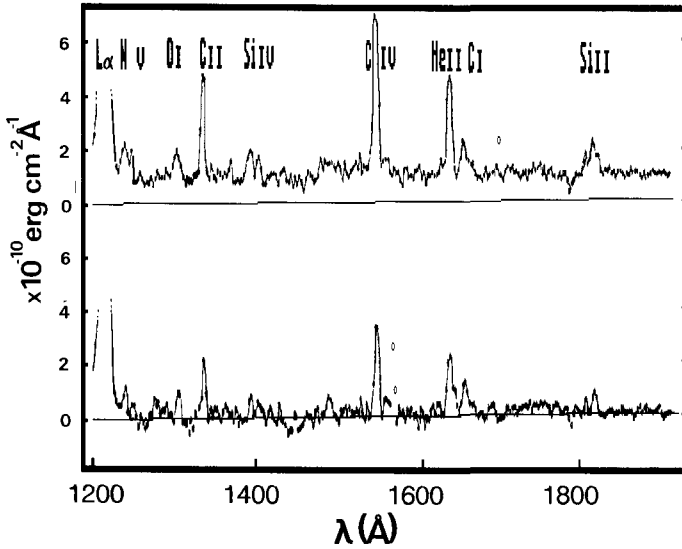


Fig. 3. An IUE short-wavelength spectrum of a flare on the dMe star, FK Aqr (a) adapted from Butler *et al.* (1981). (b) shows the star in its non-flaring state. Some of the most prominent emission lines are identified. Note the presence of a strong flare continuum.

next spectrum is of order 20 min. Since the duration of a typical UV flare appears to be much shorter than these times, no information on the time evolution of the transition region flare is possible. In spite of these restrictions, however, a great deal has been uncovered on the nature of dMe flares in the UV. Table II summarizes some of the important parameters of those stellar flares observed in the UV.

TABLE II
Summary of IUE flares

Star	Source	E_{CIV} (10^{30} erg)	EM_{CIV} (10^{52} cm $^{-3}$)	N_e (10^{11} cm $^{-3}$)	E_{TR} (10^{32} erg)	$E_{L\alpha}$ (10^{30} erg)
dMe stars						
FK Aqr	Butler <i>et al.</i> , 1981	34	(>0.05)	–	25	–
Prox Cen	Haisch <i>et al.</i> , 1983	0.5	(>0.001)	–	0.4	2.4
AT Mic	Bromage <i>et al.</i> , 1986	20	(>0.04)	≈ 10	15	40
EQ Peg	Baliunas <i>et al.</i> , 1984a	6	(>0.01)	–	4	–
AD Leo	Byrne <i>et al.</i> , 1989	0.24	(>0.001)	–	0.2	4
		2.5	(0.002)	–	2	–
YZ CMi	Rodono <i>et al.</i> , 1984	4	(>0.01)	–	3	–
RS CVn stars						
V711 Tau	Linsky <i>et al.</i> , 1988	14000	2	1	20000	1.3×10^5
λ And	Baliunas <i>et al.</i> , 1984b	> 8000	1	$1 \leq N_e \leq 10$	> 11000	55000
II Peg	Doyle <i>et al.</i> , 1989	7000	0.15	0.5	2500	–
IM Peg	Buzasi <i>et al.</i> , 1987	1×10^5	190	–	74000	–
UX Ari	Simon <i>et al.</i> , 1980	> 500	–	0.7	–	–

The resonance lines of C IV ($\lambda\lambda 1548/51 \text{ \AA}$) are the most prominent lines in the IUE short wavelength range in both quiescent and flaring spectra. Other lines seen to be enhanced during flares are those of C I ($\lambda\lambda 1657-8 \text{ \AA}$), Si II ($\lambda\lambda 1808/16/17 \text{ \AA}$), C II ($\lambda\lambda 1335/6 \text{ \AA}$), Al III ($\lambda\lambda 1856/63 \text{ \AA}$), He II ($\lambda 1640 \text{ \AA}$), Si IV ($\lambda\lambda 1394/1402 \text{ \AA}$), and N V ($\lambda\lambda 1239/43 \text{ \AA}$). In general, the degree of enhancement increases with the temperature of formation of the relevant ion, with the exception of He II. All of this is consistent with a model based on solar flares wherein the transition region is pushed to higher densities during the flare with a consequent increase in the emission measure and a steepening of its temperature dependence.

Table II lists the time integrated energy emitted by each flare in the C IV resonance lines and in other important lines, where these were observed simultaneously. Energies of $\approx 10^{31}$ erg and higher are common and such energies are comparable to those observed in soft X-rays (cf. Table I). We also list the total radiative losses from the transition region as a whole, defined by the limits, $4.2 \leq \log T_e \leq 5.4$. These have been calculated by assuming a standard flare emission measure based on a mean of a number of observed flares and the radiative loss function of Raymond, Cox, and Smith (1976). Examination of Table II shows that the total transition region emission line losses, E_{TR} , are in the region $10^{32}-10^{33}$ erg. Where simultaneous X-ray observations were made (Haisch *et al.*, 1983), the transition region losses approximately equalled those in the soft X-ray region. Similarly, where simultaneous observations of the optical line emission (Baliunas and Raymond, 1984) or $L\alpha$ emission (Bromage *et al.*, 1986; Byrne *et al.*, 1989) are available, these are also comparable to the transition region emission.

Strong UV continua have been seen in a number of dMe flares. Butler *et al.* (1981) observed a flat continuum over the entire IUE SWP range (1150–1950 \AA) during a flare on FK Aqr, while Bromage *et al.* (1986) observed a similar continuum near the peak of a flare on AT Mic which reddened later in the flare (see Figure 4). The energy contained in these continua is considerable and may be as much as any of the other loss mechanisms discussed above (see Table II). The energy in the ultraviolet continuum of the AT Mic flare was $\approx 10^5$ times that of a major solar flare.

Flares have also been observed with IUE on RS CVn stars. The most striking feature of these flares compared to those on dMes is their duration. Repeat exposures have shown C IV enhancements of about 3 over the *global* quiescent flux lasting at least 5 hours on λ And (Baliunas, Guinau, and Dupree, 1984), 7 hours on V711 Tau (Linsky *et al.*, 1988) and 6 hours on II Peg (Doyle, Byrne, and van den Oord, 1989). As a result of these long durations the energy emitted in C IV is orders of magnitude larger than in the dMes, typically $10^{34}-10^{35}$ erg. Correspondingly, the total transition region losses may be as high as $\approx 10^{37}$ erg.

It has been possible to detect electron density sensitive intersystem lines in RS CVn flare spectra, in particular C III] $\lambda 1176 \text{ \AA}$, C III] $\lambda 1909 \text{ \AA}$, and Si III] $\lambda 1893 \text{ \AA}$. Combining these derived mid-transition region electron densities with the emission measures of lines such as Si IV ($\lambda 1393/1402 \text{ \AA}$) and C IV ($\lambda 1548/51 \text{ \AA}$) has enabled some authors to derive the volumes of the flaring plasma (see Byrne *et al.*, 1987, for a description of the technique). Volumes of order $10^{29}-10^{30} \text{ cm}^3$ and electron densities of order

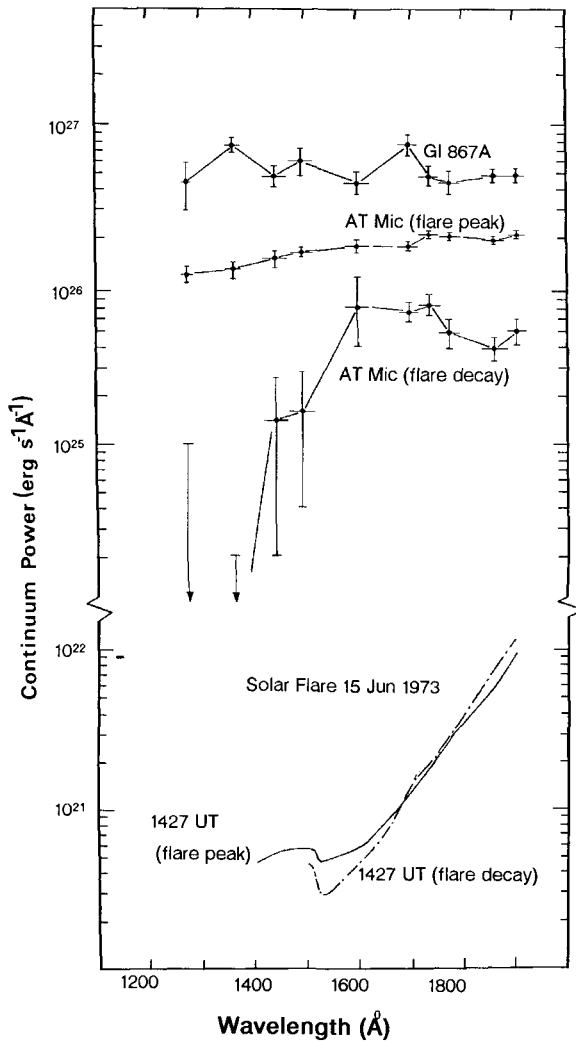


Fig. 4. A comparison of ultraviolet flare continua during two stellar flares on GI 867A (FK Aqr) and AT Mic observed in the IUE short-wavelength region and the continuum recorded in a large solar flare (Bromage *et al.*, 1986).

5×10^{10} – 10^{11} cm^{-3} are typical, not very much different from those of large solar two-ribbon flares. So it would appear that, in the transition region, RS CVn flares are more long-lived than solar or dMe flares but are otherwise fairly similar.

$L\alpha$ and MgII h & k are important sources of cooling for the upper chromospheres of both RS CVn and dMe flares. In the case of the λ And and V711 Tau flares mentioned above the $L\alpha$ and MgII losses each exceeded the total transition region losses.

4. Mass Motions

There is abundant evidence of mass motions within solar flares, ranging from $H\alpha$ surges and filament disruption to blue-shifted components in $Ca\text{XIX}$ and $Fe\text{XXV}$ during the impulsive phase. Seeking similar evidence in stellar flares is complicated by the lack of spatial and spectral resolution. Nevertheless some significant progress has been made in this area.

Recent studies of the behaviour of the Balmer line profiles with time during a flare have produced firm evidence of broadening and asymmetry. Figure 5 shows the profiles of the $H\delta$ and $H\zeta$ lines during a flare on the dMe star, YZ CMi, taken from Doyle *et al.* (1988b). Although taken from the same exposures the two lines show significantly different time evolution. The profiles taken near the peak of the flare (1) both show

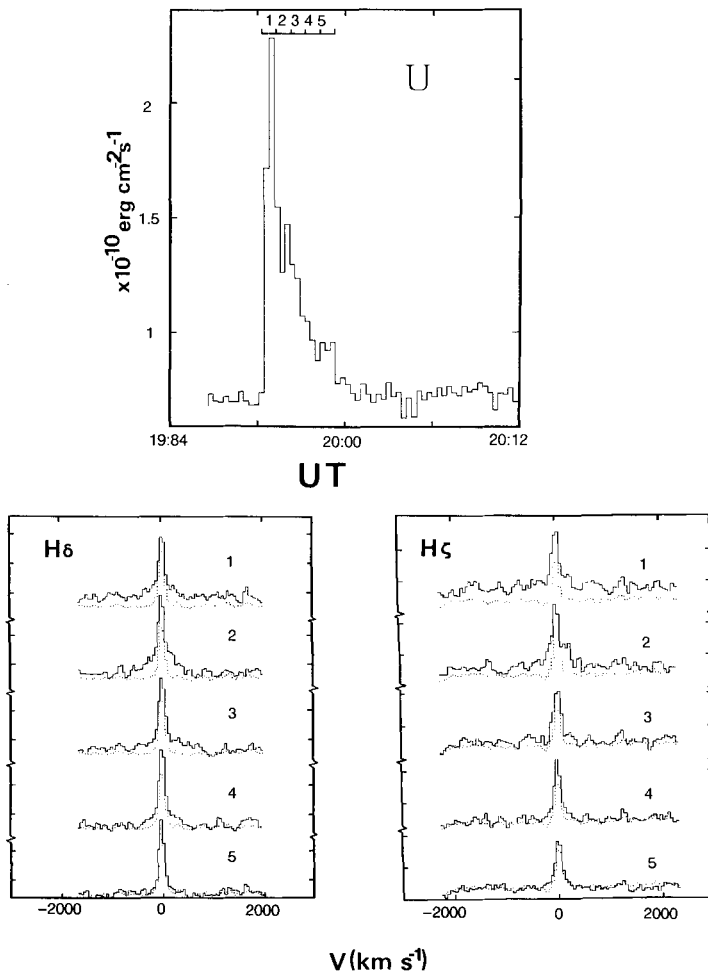


Fig. 5. Optical U -band light curve (a) and corresponding Balmer $H\delta$ (b) and $H\zeta$ (c) line profiles from a flare on ZY CMi from Doyle *et al.* (1988b). The dotted profiles in the lower panels are from a mean of several preflare spectra. The numbers refer to the time intervals during which the spectra were taken.

broadening of the core of the line compared with the mean of preflare profiles. The $H\delta$ line, however, also shows the development of significant wings. By the time of a secondary peak in the optical light curve (2) both lines have developed extended wings. The $H\delta$ wings have a pronounced redward asymmetry and extend out to $\approx 800 \text{ km s}^{-1}$. Later in the decay phase (3) these wings have weakened but they recover somewhat (4) before finally becoming unmeasurable. The excess broadening of the cores of the lines amounts to $\approx 100 \text{ km s}^{-1}$.

Although their time resolution was not as good as that of Doyle *et al.*, Phillips *et al.* (1988) found very similar results for Balmer line profiles in a flare on UV Cet. Rodono *et al.* (1989) also recorded extremely broad wings in $H\gamma$ and $H\delta$, with a pronounced red asymmetry, in a flare on AD Leo. All authors agree that the Ca II H \& K lines show a relatively weak flare response and no detectable wings or wavelength shifts.

Spectroscopy of flares on RS CVn stars has taken place mainly in the ultraviolet and, again, wavelength shifts are seen. Because of detector sensitivity limitations only the Mg II h \& k lines have been recorded at sufficiently high resolution and signal-to-noise to discuss these effects. Linsky *et al.* (1988) observed a large flare on V711 Tau with IUE and recorded the profiles of the h & k lines with a resolution of $\approx 19 \text{ km s}^{-1}$. By comparing the flare line profiles with a detailed model based on preflare data they were able to locate the flare on the K component of the binary and to derive flare-only line-profile parameters, as given in Table III. Their data were consistent with a red shift

TABLE III
Summary of wavelength shifts in dMe and RS CVn flares

Star	Source	Lines (Å)	v_{peak} (km s^{-1})	v (FWHM)	
				Core	Wings
dMe stars					
YZ CMi	Doyle <i>et al.</i> , 1988b	$H\delta$, $H\zeta$ (4101, 3889 Å)	+ 50	50	200
Wolf 630	Doyle <i>et al.</i> , 1988a	$H\alpha$ (6562 Å)	–	50	140
AD Leo	Rodono <i>et al.</i> , 1989	$H\gamma$, $H\delta$, $H\zeta$, $H\eta$ (4340, 4101, 3889, 3835 Å)	+ 30	250	750
UV Cet	Phillips <i>et al.</i> , 1988	$H\beta$, $H\gamma$ (4861, 4340 Å)	+ 100	–	–
RS CVn stars					
II Peg	Doyle <i>et al.</i> , 1989	Mg II (2796/2803 Å)	+ 25	– 30	–
V711 Tau	Linsky <i>et al.</i> , 1988	Mg II , C IV (2796/2803, 1548/51 Å)	+ 90	–	–
λ And	Baliunas <i>et al.</i> , 1984b	Mg II (2796/2803 Å)	+ 25	–	–
UX Ari	Simon <i>et al.</i> , 1980	Mg II , Fe II (2796/2803, ≈ 2600 Å)	(– 45) (+ 475)	–	–

of $\approx 90 \text{ km s}^{-1}$. Earlier IUE observations of RS CVn flares on UX Ari by Simon, Linsky, and Schiffer (1980) and on λ And by Baliunas, Guinan, and Dupree (1984) also recorded redshifted flare light in the Mg II h & k profiles. The red shifts in the UX Ari flare extended out to $\approx 475 \text{ km s}^{-1}$!

Doyle, Byrne, and van den Oord (1989) also observed a flare in the Mg II h & k lines on the RS CVn star, II Peg. In this case a preflare spectrum, taken a short time earlier and at almost the same orbital phase as the flare, was available and this was differenced with the flare spectrum to derive the Mg II profile of the flare itself. The flare was of sufficiently long duration that this was possible for two consecutive spectra of the flare. One of these profiles is given in Figure 6 with a multi-gaussian fit superimposed. There are two absorption features in the spectrum. One is also visible in the non-flare profile and is due to interstellar absorption in the line of sight. The second is intrinsic to the

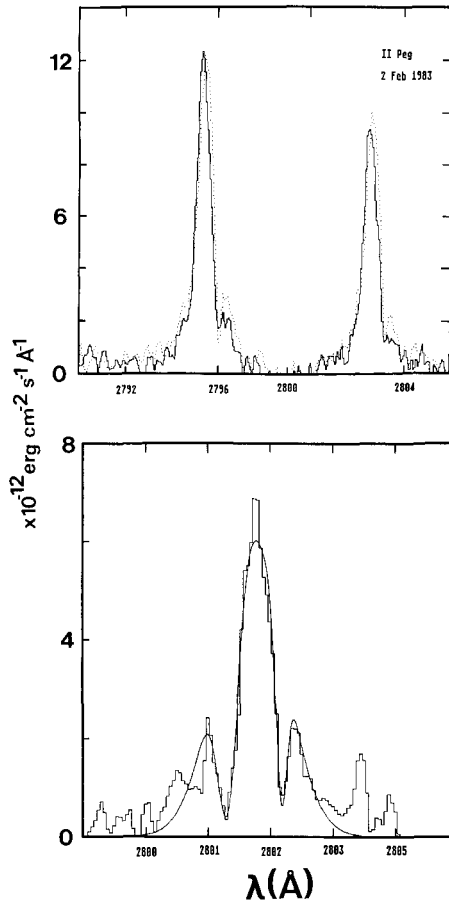


Fig. 6. The upper panel shows the Mg II h and k line profiles immediately before (solid curve) and during (broken curve) a flare on II Peg (adapted from Doyle, Byrne, and van den Oord, 1989). Note the apparent redshift of the line peak. The lower panel shows the Mg II h profile of the flare light only, after subtraction of the preflare profile and a multi-gaussian fit to this subtracted profile.

flare and apparently represents absorption by cool material overlying the flare itself. By assuming all of these components to be gaussian, the original emission profile can be reconstructed. This suggests that the Mg II emitting material in the flare was blueshifted with respect to the star by $\approx 50 \text{ km s}^{-1}$ and the absorbing material by $\approx 80 \text{ km s}^{-1}$. However, because of the effect of the absorbing material on the emission profile, the original, unsubtracted flare Mg II profile appeared slightly *redshifted* with respect to the profile of the quiescent star.

Thus, while redshifts are observed generally in both dMe and RS CVn flares, these latter high resolution observations of II Peg would indicate caution in always accepting the results of low-resolution studies of the shifts in flares.

5. Microwaves

A classic example of a multi-wavelength observation of a dMe flare, including microwaves, is the flare on AD Leo (Rodono *et al.*, 1989) shown in Figure 7. The impulsive rise in the optical *U*-band light is accompanied by a simultaneous rise in the 2 cm emission. The 6 cm emission, however, shows a much slower evolution to maximum, ≈ 10 min after the peak of the optical light. The decay time of the microwaves at both wavelengths is then comparable to the 'slow' component of the *U*-band light curve ($\tau_{\text{decay}} \approx 30$ min). This 'slow' component of the *U*-band light is known to be dominated by chromospheric emission lines, specifically the Ca II H & K and the higher H I Balmer lines. At this stage of the optical flare there is a negligible contribution from the continuum.

This pattern has been repeated in many simultaneous microwave and optical observations of flares, such as the YZ CMi flare of 3 February, 1983 (Rodono *et al.*, 1984) and another AD Leo flare on 2 February, 1983 (Gary, Byrne, and Butler, 1987). In contrast, however, an extensive study of AT Mic by Nelson *et al.* (1986) showed a very poor correlation between optical *U*-band flares and 6 cm flares. A comparable study has not been made at 2 cm, however, where the more impulsive nature of the microwave flares may make their detection easier.

Simultaneous microwave and optical observations of flares are summarized in Table IV. It will be noted in this table that there is no evident correlation between the peak flux density in microwaves and the total energy in optical or X-ray radiation. This would suggest that we are sampling a different radiating plasma at these different wavelengths.

6. Conclusions

Considerable progress has been made in the study of stellar flares, both on dMe and RS CVn stars, as a result of multi-wavelength studies of the phenomenon. The basic solar model of a localised injection of energy at the base of a magnetic loop structure and its subsequent cooling, at least in part, by radiation appears to serve us well for stellar flares also.

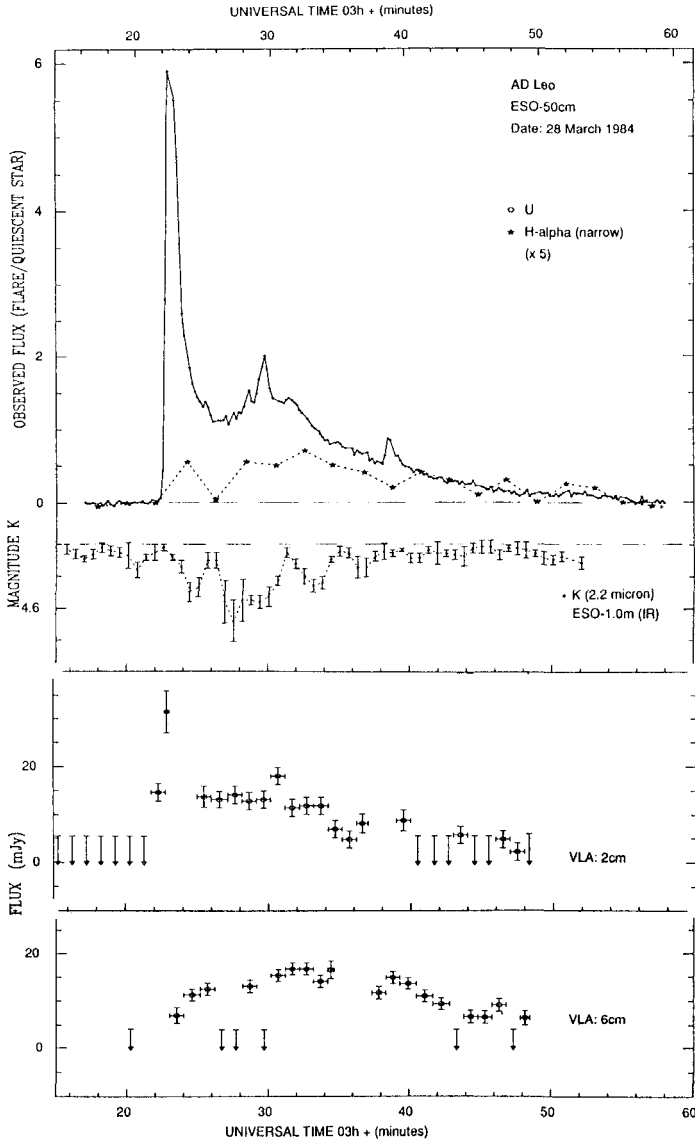


Fig. 7. Simultaneous optical (*UBVRI*), infrared (*K*-band) and microwave (2 and 6 cm) observations of a large flare on AD Leo from Rodono *et al.* (1989).

Table V summarizes what we consider the most reasonable average parameters of stellar flares to be based on the observational survey made here. It will be noted from this table that the basic parameters of the dMe star flares are not of a different order of magnitude to solar flares except in mean energy per flare. In the case of the RS CVn stars, however, this is not the case. Evidently the binary nature of the RS CVs, combined with their lower gravities, is capable of boosting the energy content per flare. Whether this occurs through a more efficient dynamo mechanism or more efficient magnetic flux

TABLE IV
Summary of microwave flares on dMe stars

Star	Source	S (2 cm) (mJy)	S (6 cm) (mJy)	S (20 cm) (mJy)	E_X (10^{30} erg)	E_{opt} (10^{30} erg)
UV Cet	Kundu <i>et al.</i> , 1988	–	2.8	10	6	–
		–	3	35	3	–
AT Mic	Nelson <i>et al.</i> , 1986	–	17	–	–	70
EQ Peg	Kundu <i>et al.</i> , 1980	–	> 12	> 10	10^4	–
AD Leo	Byrne <i>et al.</i> , 1989 Kundu <i>et al.</i> , 1988 Rodono <i>et al.</i> , 1984	–	3	–	–	15 (U)
		–	4.5	–	?	–
		32	16	–	–	300 (U)
YZ CMi	Rodono <i>et al.</i> , 1989 Kundu <i>et al.</i> , 1988	< 2	5.5	< 2	–	200 (U)
		–	2	15	20	–

TABLE V
Summary of dMe and RS CVn flare parameters

	dMe	RS CVn
Soft X-ray emission measure (cm^{-3})	10^{51} – 10^{53}	10^{53} – 10^{54}
X-ray temperature (K)	1 – 5×10^7	6 – 10×10^7
X-ray electron density ($\tau_{1/2}$) (cm^{-3})	1 – 8×10^{11}	3 – 9×10^{11}
Integrated energy (erg)	10^{31} – 10^{34}	10^{34} – 10^{36}
CIV emission measure (cm^{-3})	10^{49} – 2×10^{50} (?)	10^{51} – 10^{54}
Transition region electron density (cm^{-3})	$\leq 10^{12}$	5 – 10×10^{10}
Integrated transition region energy (erg)	10^{31} – 10^{33}	10^{35} – 10^{37}
Line peak velocities (km s^{-1})	+ 30–+ 50	+ 25–+ 90
Turbulent velocities (km s^{-1})	50–250	60–120

concentration or some other means of tapping the orbital energy of the binary is not yet clear. What is clear is that continued multi-wavelength studies of the flare phenomenon can contribute to a better understanding of the phenomenon.

References

- Baliunas, S. L. and Raymond, J. C.: 1984a, *Astrophys. J.* **282**, 728.
 Baliunas, S. L., Guinan, E. F., and Dupree, A. K.: 1984b, *Astrophys. J.* **282**, 733.
 Bromage, G. E., Phillips, K. J. H., Dufton, P. L., and Kingston, A. E.: 1986, *Monthly Notices Roy. Astron. Soc.* **220**, 1021.
 Butler, C. J., Rodono, M., and Foing, B. H.: 1989, *Astron. Astrophys.* (in press).
 Butler, C. J., Byrne, P. B., Andrews, A. D., and Doyle, J. G.: 1981, *Monthly Notices Roy. Astron. Soc.* **197**, 815.
 Buzasi, D. L., Ramsey, L. W., and Huenemoerder, D. P.: 1987, *Astrophys. J.* **322**, 353.
 Byrne, P. B., Doyle, J. G., Brown, A., Linsky, J. L., and Rodono, M.: 1987, *Astron. Astrophys.* **180**, 172.
 Byrne, P. B., Brown, A., Butler, C. J., Gary, D. E., Linsky, J. L., and Simon, T.: 1989, *Astron. Astrophys.* (in preparation).
 Cohen, L., Feldman, U., and Doschek, G. A.: 1978, *Astrophys. J. Suppl.* **37**, 393.
 De Jager, C., Heise, J., Avagoloupis, S., Cutispoto, G., Kieboom, K., Herr, R. B., Landini, M., Langerwerff,

- A. F., Mavridis, L. N., Melikian, A. S., Molenaar, R., Monsignori-Fossi, B. C., Nations, H. L., Pallavicini, R., Pirola, V., Rodono, M., Seeds, M. A., van den Oord, G. H. J., Vilhu, O., and Waelkins, C.: 1988, *Astron. Astrophys.* **156**, 95.
- Doyle, J. G., Byrne, P. B., and van den Oord, G. H. J.: 1989, *Astron. Astrophys.* (in press).
- Doyle, J. G., Butler, C. J., Callinan, P. J., Tagliaferri, G., de la Reza, R., Torres, C. A., and Quast, G.: 1988a, *Astron. Astrophys.* **191**, 79.
- Doyle, J. G., Butler, C. J., Byrne, P. B., and van den Oord, G. H. J.: 1988b, *Astron. Astrophys.* **193**, 229.
- Gary, D. E., Byrne, P. B., and Butler, C. J.: 1987, in J. L. Linsky and R. E. Stencel (eds.), *Cool Stars, Stellar Systems and the Sun*, Proc. 5th Cambridge Workshop on Cool Stars, p. 106.
- Haisch, B. M., Linsky, J. L., Slee, O. B., Siegman, B. C., Nikoloff, I., Candy, H., Harwood, D., Verveer, A., Quinn, P. J., Wilson, I., Page, A. A., Higson, P., and Seward, F. D.: 1981, *Astrophys. J.* **245**, 1009.
- Haisch, B. M., Linsky, J. L., Bornman, P. L., Antiochos, S. K., Golub, L., and Vaiana, G. S.: 1983, *Astrophys. J.* **267**, 280.
- Haisch, B. M., Butler, C. J., Doyle, J. G., and Rodono, M.: 1987, *Astron. Astrophys.* **181**, 96.
- Kahler, S. et al.: 1982, *Astrophys. J.* **252**, 239.
- Kundu, M. R., Pallavicini, R., White, S. M., and Jackson, P. D.: 1988, *Astron. Astrophys.* **195**, 159.
- Linsky, J. L., Neff, J. E., Brown, A., Gross, B. D., Simon, T., Andrews, A. D., Rodono, M., and Feldman, P. A.: 1988, *Astron. Astrophys.* **211**, 173.
- Neidig, D.: 1988, *Solar Phys.* **121**, 261 (this issue).
- Nelson, G. J., Robinson, R. D., Slee, O. B., Ashley, M. C. B., Hyland, A. R., Touhy, I. R., Nikoloff, I., and Vaughan, A. E.: 1986, *Monthly Notices Roy. Astron. Soc.* **220**, 91.
- Phillips, K. J. H., Bromage, G. E., Dufton, P. L., Keenan, F. P., and Kingston, A. E.: 1988, *Monthly Notices Roy. Astron. Soc.* **235**, 573.
- Raymond, J. C., Cox, D. P., and Smith, B. W.: 1976, *Astrophys. J.* **204**, 290.
- Rodono, M., Cutispoto, G., Catalano, S., Linsky, J. L., Gibson, D. M., Brown, A., Haisch, B. M., Butler, C. J., Byrne, P. B., Andrews, A. D., Doyle, J. G., Gary, D. E., Henry, G. W., Russo, G., Vittone, A., Scaltriti, F., and Foing, B.: 1984, *Proc. 4th European IUE Conf.*, ESA SP-218, p. 247.
- Rodono, M., Houdebine, E., Catalano, S., Foing, B., Butler, C. J., Scaltriti, F., Cutispoto, G., Gary, D. E., and Gibson, D. M.: 1989, *Proc. IAU Colloq. 104 – Poster Papers*, Reprints Catania Obs. (in press).
- Simon, T., Linsky, J. L., and Schiffer, F. H.: 1980, *Astrophys. J.* **239**, 911.
- Schmitt, J. H., Lemen, J. R., and Zarro, D.: 1989, *Solar Phys.* **121**, 361 (this issue).
- Tanaka, K., Nitta, N., Akita, K., and Watanabe, T.: 1983, *Solar Phys.* **86**, 91.
- van den Oord, G. H. J., White, N. E., Culhane, J. L., Parmar, A. N., Kellett, B. J., Kahn, S., and Kuijpers, J.: 1986, *Astrophys. J.* **301**, 262.
- van den Oord, G. H. J., Mewe, R., and Brinkman, A. C.: 1988, *Astron. Astrophys.* **205**, 181.